

A Geometrical Model for Arrayed Waveguide Grating based Optical Multiplexer/Demultiplexer

Dasan Meena^{1, 2, *}, Orappanpara S. Sunishkumar³, Devendra C. Pande²,
Talabattula Srinivas¹, Vadake K. Jayasree³, Fredy Francis³,
Kundil T. Sarath³, and Elambilayi Dipin³

Abstract—This paper mathematically models the operation of Arrayed Waveguide Grating (AWG) based multiplexer (mux) and demultiplexer (demux) used in optical networks. In WDM networks, the optical mux and demux play a crucial role of managing the aggregation and segregation of wavelengths for networking applications. A simple and intuitive model of AWG based mux design is discussed in this work. This model assumes that the device is linear, in which the principle of superposition is valid, and the primary emphasis is given to the optical power gain of the individual wavelengths. By using this model, one can exactly estimate the individual and overall power associated with each of the multiplexed wavelengths. The developed model was evaluated with experimental results using AWG based multiplexers. The experiments were repeated for different test cases with various power input levels and multiplexer configurations. It was found that the developed model provided a good approximation to the actual AWG mux/demux.

1. INTRODUCTION

Wavelength Division Multiplexing (WDM) systems can simultaneously carry multiple high-speed data channels over a conventional single-mode optical fibre. This increases the data transmission capacity of the fibre manifold, without altering the modulation characteristics of the individual channels, or adding significant hardware complexity. Further, WDM systems allow for more flexible network architectures, which can make use of wavelength routers and/or add-drop multiplexers (ADM) [1]. The wavelength multiplexers and demultiplexers, which combine and separate wavelengths along the link are key components in WDM systems. In fact, many design constraints are specified by the WDM mux/demux characteristics.

The Arrayed Waveguide Grating (AWG), also referred to as Phased Array Grating (PHASARS), is commonly used as multiplexer/demultiplexer in WDM systems because of its low insertion loss, high stability, flatter pass band, low cost and ease to implement in an integrated optic substrate [2]. AWG mainly consists of a waveguide array, input and output waveguides and the two Free Propagation Regions (FPRs). The input and output waveguides are arranged in a Rowland type where ends are uniformly located in a circle. This paper brings out a simple and intuitive mathematical model of an AWG based mux and demux which can be effectively used in the optical network design and applications.

Wavelength demultiplexers, since the early 1990s, have focused on grating-based and Phased Array based devices, [PHASAR] [3] which are imaging devices that disperse the input into spatially separate output foci. The main difference between the two is that grating-based devices use vertical gratings (reflective/transitive) for dispersion and focusing, while the PHASARS uses an array of waveguides, with

Received 19 January 2014, Accepted 4 March 2014, Scheduled 14 March 2014

* Corresponding author: Meena Dasan (meenad@ece.iisc.ernet.in).

¹ Indian Institute of Science (IISc), Bangalore, India. ² Electronics and Radar Development Establishment (LRDE), DRDO (Ministry of Defence), Bangalore, India. ³ Electronics and Communication Engineering, Model Engineering College, Kochi, India.

length chosen properly to provide required dispersion and imaging. The grating etching process can thus be avoided in PHASARS, which makes the device more desirable in integrated optical applications.

Phased arrays were proposed by Smit in 1988 [4]. He succeeded in manufacturing a small 1×5 demultiplexer having channel spacing of 0.5% working in the He-Ne laser wavelength. It showed good focusing and a channel separation of 20 dB. It used a concentric bend waveguides approach making the wavelength resolution poor (several nm). Later Vellekoop and Smit modified this by adding a coupler and an adapter section, which reduced the loss significantly. The developed device worked at 633-nm with a dimension of $0.6 \times 2.5 \text{ mm}^2$. They found the attenuation to be as low as 0.5 dB and crosstalk of the order 17–21 dB [5]. Meanwhile, the longer wavelength version of AWG was developed by Takahashi et al. [6]. They used arrayed waveguides of different length and same curvature radius. This enabled use of longer waveguide path difference of AWG fibres and was thus able to obtain a higher frequency resolution. Later Dragone et al. expanded $1 \times N$ AWG device to an $N \times N$ device, namely the wavelength router, mainly used in multiwavelength network applications [7]. Zirngibl et al. developed InP-based PHASAR-Demux, in 1992, which was suitable for photonic integrated circuits due to their higher refractive index contrast [8].

The existing AWG mux/demux theory is based on diffraction and imaging properties. The output is taken as an image of the input at each output waveguides, after going through a region of free space propagation, which is to be analyzed based on basic electromagnetic theory and diffraction [3]. This work focuses on developing an approximate but effective geometrical approach for AWG design based on trigonometric principles. This model can be considered as a geometrical approximation of AWG analysis using the classical ray and wave theories. The signal power is the sole parameter here, and analysis is based on power division and superposition principles.

Although [3] provided a precise mathematical derivation of the phase matching condition, the present approach stands out in making use of a simplistic geometrical analysis of the Rowland and Grating circle construction based on scalene triangles in deriving the phase match condition.

2. AWG BASICS AND OPERATION

AWG Mux is a generalized form of the Mach-Zehnder Interferometer (MZI) [7]. MZI is a device in which two copies of same signals are shifted by a certain phase and then added together. But, in AWG several phase shifted copies of the same signal are added together.

The AWG consists of a waveguide array, an input and output waveguides and two Free Propagation Regions (FPRs) as shown in Figure 1 [9]. The input and output waveguides are structured on the arc of a “Rowland circle” and the arrayed waveguides are located on the arc of a circle called the “grating circle”, as shown in Figure 2.

Let the number of input and output waveguides of AWG be denoted by ‘ n ’. The input and output couplers are of $n \times m$ and $m \times n$ size, respectively. Thus there will be ‘ m ’ number of arrayed waveguides, which interconnects the two couplers. The difference in length between the consecutive waveguides is a constant denoted by ‘ ΔL ’. The first coupler splits the input optical signal into ‘ m ’ parts. The relative phases of these split signals depend on the distance travelled by the signal in the coupler from an input

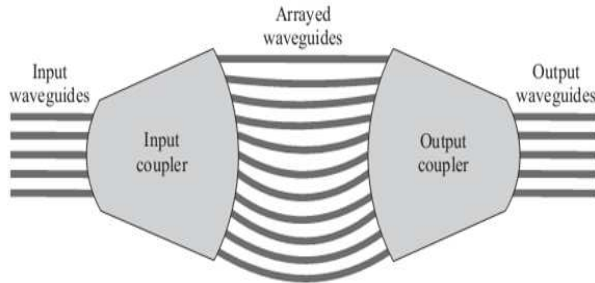


Figure 1. Arrayed waveguide grating.

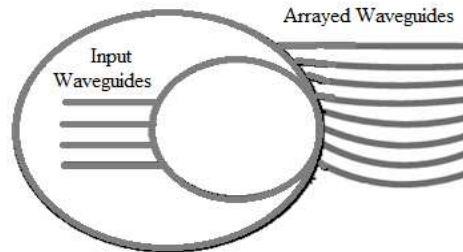


Figure 2. Rowland circle and grating circle.

waveguide to the arrayed waveguide.

Let d_{ik}^{in} represent the difference in distance travelled from an input waveguide ‘ i ’ to an arrayed waveguide ‘ k ’. Similarly, d_{kj}^{out} represents difference in distance travelled from an arrayed waveguide ‘ k ’ to an output waveguide ‘ j ’. The relative phase of signal from input ‘ i ’ to output ‘ j ’ traversing ‘ k th’ arrayed waveguide between them, is given by,

$$\phi_{ijk} = \frac{2\pi}{\lambda} (n_1 d_{ik}^{in} + n_2 k \Delta L + n_1 d_{kj}^{out}) \quad \text{where } k = 1, 2, \dots, m \quad (1)$$

where ‘ n_1 ’ is the refractive index of input and output directional coupler regions, ‘ n_2 ’ the refractive index of arrayed waveguide region, and ‘ ΔL ’ the length difference between consecutive arrayed waveguides. From the input waveguide ‘ i ’, those wavelengths ‘ λ ’, for which ‘ ϕ_{ijk} ’ differ by multiple of 2π , will add in phase at the output waveguide ‘ j ’ [2, 10].

The input and output couplers can be designed such that,

$$d_{ik}^{in} = d_i^{in} + k \partial_i^{in} \quad \text{and} \quad d_{kj}^{out} = d_j^{out} + k \partial_j^{out} \quad (2)$$

where ‘ ∂_i^{in} ’, ‘ ∂_j^{out} ’ are the distances travelled in input and output coupler regions, respectively.

Therefore,

$$\phi_{ijk} = \frac{2\pi}{\lambda} (n_1 d_i^{in} + n_1 d_j^{out}) + \frac{2\pi k}{\lambda} (n_1 \partial_i^{in} + n_2 \Delta L + n_1 \partial_j^{out}) \quad (3)$$

For the use as a mux and demux, the AWG should satisfy the following relation [11, 12]

$$n_1 \partial_i^{in} + n_2 \Delta L + n_1 \partial_j^{out} = p \lambda_j \quad (4)$$

where ‘ p ’ is an integer.

In the above equation if a wavelength λ_j satisfies

$$n_1 \partial_i^{in} + n_2 \Delta L + n_1 \partial_j^{out} = (p + 1) \lambda'_j \quad (5)$$

Then both ‘ λ_j ’ and λ'_j are demultiplexed at output port ‘ j ’ from input port ‘ i ’.

3. PROPOSED MATHEMATICAL MODEL

3.1. AWG as Multiplexer

The coupler in AWG is a 3 dB coupler. Therefore, the same copy of the input wavelengths appears on all the arrayed waveguides. Let ‘ $p_{(\lambda_i)}$ ’ be the power at each wavelength ‘ λ_i ’, where $i = 1, 2, \dots, n$. As we know, there are ‘ m ’ number of arrayed waveguides then the power ‘ $p_{(\lambda_i)}$ ’ is equally divided into ‘ m ’ parts. Each part can be denoted as $p'_{(\lambda_i)}$. An AWG configured as multiplexer is shown in Figure 3.

As per the theory of AWG, the waveguide lines that satisfy condition (4) will be added together to get resultant power at output port ‘ j ’. Therefore, a finite number (depends on Rowland circle geometry) of copies of power $p'_{(\lambda_i)}$ will add in phase and that will be the average optical power at that particular wavelength ‘ λ_i ’. Here, we assume that the device is linear, where the principle of superposition is valid.

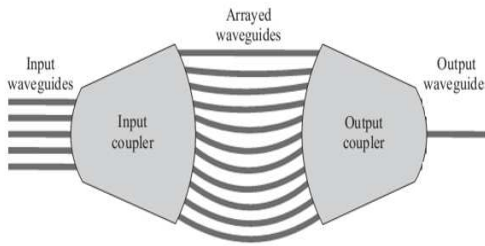


Figure 3. Arrayed waveguide grating as multiplexer.

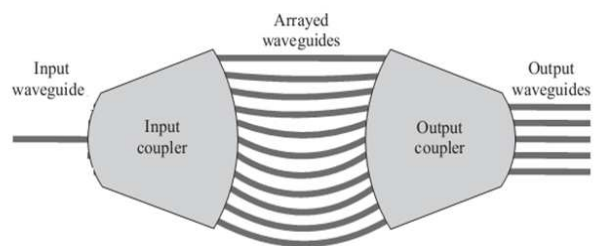


Figure 4. Arrayed waveguide grating as demultiplexer.

The total output optical power from the output port of the AWG is equal to the algebraic sum of all individual powers corresponding to each ' λ_i '. Therefore,

$$P_{out} = \sum_{i=1}^n a_i p''_{(\lambda_i)} \quad (6)$$

where ' a_i ' is the signal attenuation, $p''_{(\lambda_i)}$ the total power corresponding to each ' λ_i ' at the output port, and $p'_{(\lambda_i)}$ the sum of all the copies of $p'_{(\lambda_i)}$ in which the corresponding waveguide line satisfies the condition given in Equation (4).

$p''_{(\lambda_i)}$ depends on the number of arrayed waveguide lines, the difference in length ' ΔL ' and radius ' R ' of the Rowland circle. Then,

$$P''_{(\lambda_i)} = \sum_{k=1}^{l_i} b_k p'_{(\lambda_{ik})} \quad (7)$$

where ' l_i ' is the number of waveguide lines satisfying the condition (4), ' b_k ' the attenuation of ' k th' waveguide, and $p'_{(\lambda_{ik})}$ the power corresponding to ' k th' copy of ' λ_i '.

If there are ' n ' number of wavelengths, then the input optical power corresponding to each wavelength is denoted by $p_{(\lambda_i)}$. Therefore, the power ratio between output and input for each wavelength can be denoted as,

$$\frac{P_{out}(\lambda_i)}{P_{in}(\lambda_i)} = \frac{\sum_{k=1}^{l_i} b_k p'_{(\lambda_{ik})}}{p_{(\lambda_i)}} \quad (8)$$

Total output power to each input wavelength is given by,

$$P_{MUX} = \frac{\sum_{i=1}^n a_i p''_{(\lambda_i)}}{p_{(\lambda_i)}} = \frac{\sum_{i=1}^n a_i \left[\sum_{k=1}^{l_i} b_k p'_{(\lambda_{ik})} \right]}{p_{(\lambda_i)}} \quad (9)$$

Since the coupler is a 3 dB coupler, all the copies of $p'_{(\lambda_i)}$ are the same. Then,

$$\sum_{k=1}^{l_i} b_k p'_{(\lambda_{ik})} = \sum_{k=1}^{l_i} b_k l_i p'_{(\lambda_i)} = l_i \sum_{k=1}^{l_i} b_k p'_{(\lambda_i)} \quad \therefore P_{MUX} = \frac{\sum_{i=1}^n a_i l_i \left[\sum_{k=1}^{l_i} b_k p'_{(\lambda_i)} \right]}{p_{(\lambda_i)}} \quad (10)$$

when ' b_k ' is negligible

$$P_{MUX} = \frac{\sum_{i=1}^n a_i l_i p'_{(\lambda_i)}}{p_{(\lambda_i)}} \quad (11)$$

3.2. AWG as Demultiplexer

The condition for demultiplexing is according to Equation (4), which is the same as the operation of multiplexer. There, the total input optical power is the sum of the optical powers of individual wavelengths. An AWG configured as demultiplexer is shown in Figure 4.

Let ' $p_{(\lambda_i)}$ ' be the power for the wavelength ' λ_i '. Then the total input power is given by

$$P_{(\lambda)} = \sum_{i=1}^n p_{(\lambda_i)} \quad (12)$$

In the input ($1 \times m$) coupler this signal power ' $P_{(\lambda)}$ ' is split into ' m ' parts, and each part is denoted as $P'_{(\lambda)}$.

Depending upon the condition (4), there are a finite number of copies of $P'_{(\lambda_i)}$, which will add in-phase and will be the power corresponding to ' λ_i ' at the output.

Let $P_{(\lambda_i)out}$ be the component power associated with wavelength ' λ_i ', then

$$P_{(\lambda_i)out} = \sum_{k=0}^{l_i} b_k p'_{(\lambda_{ik})} = l_i \sum_{k=0}^{l_i} b_k p'_{(\lambda_i)} \tag{13}$$

Therefore, the ratio of power between each output wavelength ' λ_i ' and the total input power is given by

$$P_{DEMUX(i)} = \frac{P_{(\lambda_i)out}}{P_{(\lambda)}} = \frac{l_i \sum_{k=0}^{l_i} b_k p'_{(\lambda_i)}}{\sum_{i=1}^n p_{(\lambda_i)}} \tag{14}$$

3.3. Geometric Analysis of AWG Model

The wavelength dependency of an AWG is an important factor that has to be considered during design. It depends on the physical dimensions of AWG. For exact analysis, the geometric modeling of the FPR and Arrayed Waveguide is required. The physical construction of FPR is based on the Rowland circle as shown in Figure 5.

From (4) the value of ' ΔL ' is given by

$$\Delta L = m \frac{\lambda_c}{n_{eff}} \tag{15}$$

where m is the order of the array, ' λ_c ' the central wavelength of AWG, and ' n_{eff} ' the effective refractive index of the guided mode. This length increment ' ΔL ' of the array gives rise to a phase difference according to

$$\Delta\phi_1 = \beta \Delta L \tag{16}$$

where, propagation constant, $\beta = 2\pi v \frac{n_{eff}}{c}$ and $v = \frac{c}{\lambda}$. So $\beta = 2\pi \frac{c}{\lambda} \frac{n_{eff}}{c}$.

By removing ' c ' we get,

$$\beta = 2\pi \frac{n_{eff}}{\lambda} \tag{17}$$

$$\Delta\phi_1 = 2\pi \Delta L \left(\frac{n_{eff}}{\lambda} \right)$$

The phase matching at the imaging plane of the AWG depends on the combined path length of the arrayed waveguide and the distance between each input and output waveguides and the arrayed waveguide in the two FPRs.

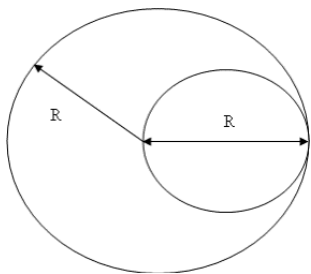


Figure 5. Grating circle and Rowland circle.

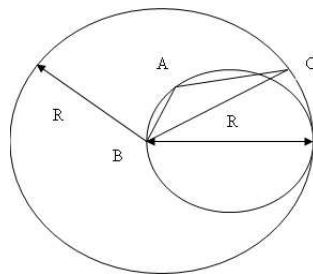


Figure 6. Scalene triangle inside Rowland circle.

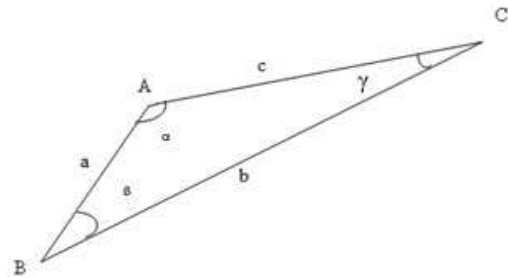


Figure 7. Scalene triangle.

The geometry for finding this FPR distance is obtained by considering the ‘scalene triangle’ formed inside the FPR as shown in Figure 6.

Consider the triangle ABC, Figure 7.

According to law of cosines

$$a^2 = b^2 + c^2 - 2bc \cos \alpha \quad (18)$$

$$b^2 = a^2 + c^2 - 2ac \cos \beta \quad (19)$$

$$c^2 = a^2 + b^2 - 2ab \cos \gamma \quad (20)$$

We can find the length ‘a’ by considering the Rowland circle inside the grating circle as shown below.

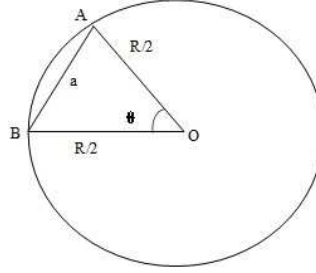


Figure 8. Rowland circle.

Consider the triangle $\triangle ABO$ inside Rowland circle (Figure 8) where ‘a’ is given by

$$a = 2 \frac{R}{2} \sin \theta/2 \quad (21)$$

Therefore

$$a = R \sin \theta/2 \quad (22)$$

Consider (20) where $b = R$ and $a = R \sin \theta/2$, substitute in Equation (20) then

$$c^2 = R^2 + R^2 \sin^2 \theta/2 - 2R^2 \sin \theta/2 \cos \gamma \quad (23)$$

$$c = \sqrt{R^2 (1 + \sin^2 \theta/2 - 2 \sin \theta/2 \cos \gamma)} \quad (24)$$

$$\therefore c = R [1 + \sin^2 \theta/2 - 2 \sin \theta/2 \cos \gamma]^{1/2} \quad (25)$$

Therefore, the total phase shift of the signal propagating through a distance ‘c’ is given by,

$$\Delta \phi_2 = \frac{2\pi}{\lambda} c \quad (26)$$

$$\therefore \Delta \phi_2 = \frac{2\pi}{\lambda} R [1 + \sin^2 \theta/2 - 2 \sin \theta/2 \cos \gamma]^{1/2} \quad (27)$$

If the total phase shift of the copies of optical signal after propagating through two FPRs and Arrayed Waveguide is a multiple of 2π , then the constructive interference will occur at the imaging plane of the second FPR. That is

$$\Delta \phi_1 + 2\Delta \phi_2 = n2\pi \quad (28)$$

where ‘n’ is an integer. From (17) and (27),

$$2\pi \Delta L \left(\frac{n_{eff}}{\lambda} \right) + \frac{4\pi}{\lambda} R [1 + \sin^2 \theta/2 - 2 \sin \theta/2 \cos \gamma]^{1/2} = n2\pi$$

$$\text{Or } \Delta L \left(\frac{n_{eff}}{\lambda} \right) + \frac{2}{\lambda} R [1 + \sin^2 \theta/2 - 2 \sin \theta/2 \cos \gamma]^{1/2} = n \quad (29)$$

$$\text{Taking } \frac{1}{\lambda} \text{ outside } \frac{1}{\lambda} [\Delta L n_{eff} + 2R [1 + \sin^2 \theta/2 - 2 \sin \theta/2 \cos \gamma]^{1/2}] = n$$

$$\therefore \Delta L n_{eff} + 2R [1 + \sin^2 \theta/2 - 2 \sin \theta/2 \cos \gamma]^{1/2} = n\lambda \quad (30)$$

The above condition is used for the constructive interference modeling of various wavelengths at the output of the mux during AWG modeling. The first term corresponds to the array waveguide regions and the second represents the effect of two FPRs.

The parameter ‘ l_i ’ (in Equation (11)) and the number of waveguide lines satisfying Equation (4) can be obtained by using above derived Equation (30).

3.4. AWG Model Evaluation

After obtaining ‘ l_i ’ for each wavelength and using the descriptions mentioned under Section 3.1, the total output power of AWG based multiplexer is modeled. Wavelength dependent power is computed using Equation (7). The model is evaluated in a standard simulation environment. Further, these results are evaluated against experimental results for different test cases, with various input power levels and AWG configurations.

The attenuation values will depend on the spatial distribution of ports under consideration on the circumference of Rowland and grating circles. The output power of Mux will vary with respect to these attenuation values and number of arrayed waveguides, which in turn affects ‘ l_i ’. But these parameters are usually not available with commercial AWGs. Therefore, during the evaluation process, an empirical relation was derived from the experimental observations. Thus, the total mux output power is given by the empirical formula, proved by mathematical induction is,

$$P_{out}(\lambda_i) = \begin{cases} |(\lambda_c - \lambda_i)| \times \left(\frac{n'}{m}\right) \frac{P_{\lambda_i}}{|(\lambda_c - \lambda_i)|} & \text{for } \lambda_i \neq \lambda_c \\ 1.5 \times \left(\frac{n'}{m}\right) \frac{P_{\lambda_i}}{|(\lambda_c - \lambda_i + 1)|} & \text{for } \lambda_i = \lambda_c \end{cases} \quad (31)$$

Therefore,

$$P_{out}(\lambda_i) = \begin{cases} \left(\frac{n'}{m}\right) P_{\lambda_i} & \text{for } \lambda_i \neq \lambda_c \\ 1.5 \times \left(\frac{n'}{m}\right) P_{\lambda_i} & \text{for } \lambda_i = \lambda_c \end{cases} \quad (32)$$

where n' is the number of copies of P_{λ_i} satisfying the phase match condition, ‘ m ’ the number of arrayed waveguides, ‘ λ_c ’ AWG center wavelength, and ‘ λ_i ’ represents each of the input wavelengths.

4. EXPERIMENTAL SETUP

The following section discusses the experimental set up used for the evaluation of AWG based multiplexer models. It consists of laser sources, AWG based multiplexer and a power meter for the measurement of

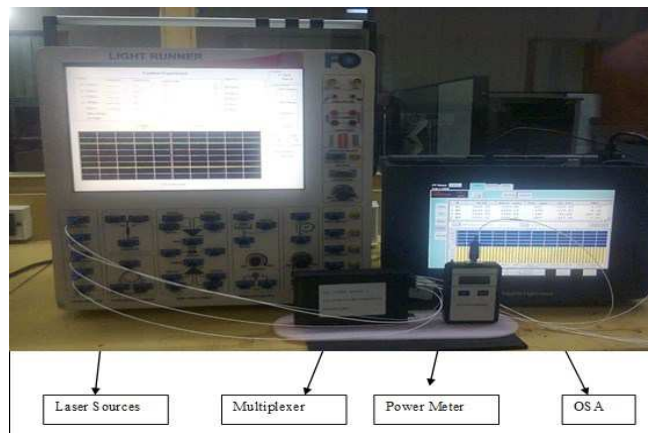


Figure 9. Experimental setup.

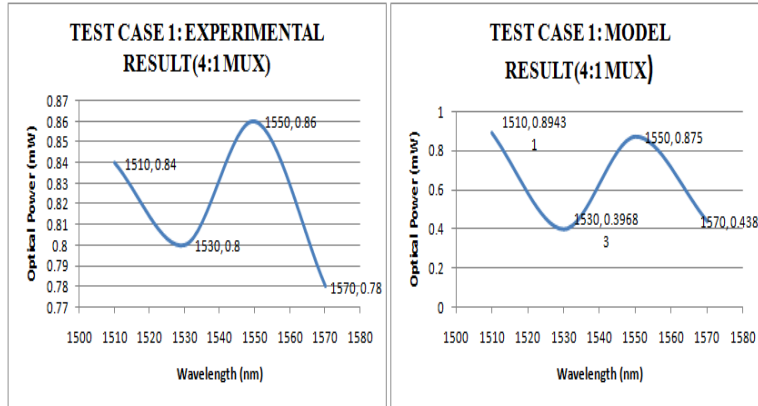


Figure 10. Comparative result (4 : 1 mux).

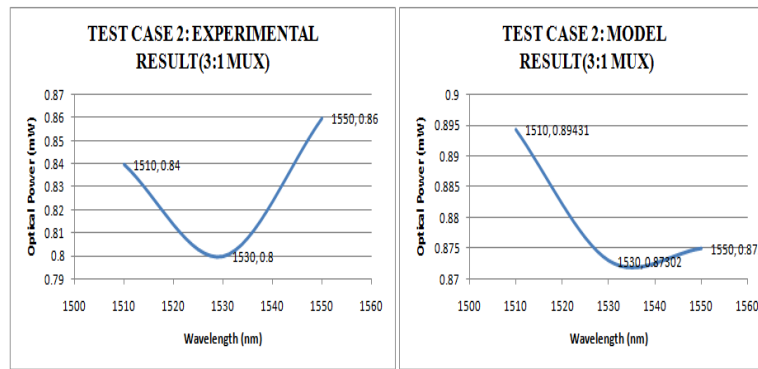


Figure 11. Comparative result (3 : 1 mux).

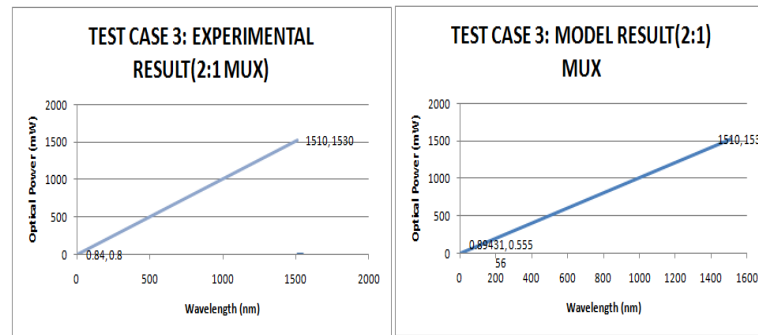


Figure 12. Comparative result (2 : 1 mux).

power output levels. The four independent laser sources are tuned for four different wavelengths 1510 nm, 1530 nm, 1550 nm and 1570 nm, respectively. Further, the experiments are repeated for various test cases with different power levels using modulated laser outputs of around 1 mW and 0.85 mW, respectively. A digital input of frequency of 2.4 MHz and 50% duty cycle is directly modulating the laser outputs. The modeling of direct modulated lasers is not included within the scope of the present work. More emphasis is given for the modeling of AWG based multiplexer. Similarly, experiments are repeated for various multiplexer configurations such as 2 : 1, 3 : 1 and 4 : 1.

Figure 9 shows the experimental set up. The setup consists of sources which produces four different wavelengths, a commercial AWG based mux and a power meter. Further, the output of mux is also monitored on an Optical Spectral Analyzer (OSA) to obtain wavelength dependent power output.

5. RESULTS

Tables 1 and 2 show the results obtained during mathematical model analysis and corresponding experimental results for similar test case input power levels. They also give results for various multiplexer configurations. We can observe that the model results are comparable with experimental results.

Figures 10, 11 and 12 show the wavelength dependent power output plots at the output of the multiplexer for various test cases. These power values are further used for the computation of total power output.

Table 1. Test case results (1 mW) I/P power for various mux configurations.

EXPERIMENTAL RESULTS		MODEL RESULTS	
TEST CASE 1 (4 : 1 MUX)		TEST CASE 1 (4 : 1 MUX) TOLERANCE LEVEL 0.5	
WAVELENGTH (nm)	POWER (mW)	WAVELENGTH (nm)	POWER (mW)
1510	0.84	1510	0.89431
1530	0.8	1530	0.39683
1550	0.86	1550	0.875
1570	0.78	1570	0.4386
MUX OUTPUT	2.2	MUX OUTPUT	2.6047
TEST CASE 2 (3 : 1 MUX)		TEST CASE 2 (3 : 1 MUX) 0.5	
1510	0.84	1510	0.89431
1530	0.8	1530	0.87302
1550	0.86	1550	0.875
MUX OUTPUT	1.55	TOTAL POWER	2.6423
TEST CASE 3 (2 : 1 MUX)		TEST CASE 3 (2 : 1 MUX)	
1510	0.84	1510	0.89431
1530	0.8	1530	0.55556
MUX OUTPUT	1.09	TOTAL POWER	1.4499

Table 2. Test case results (2.45 MHz modulated and 0.85 mW) I/P power for mux configurations.

EXPERIMENTAL RESULT (MOD WITH 2.45 MHz)		MODEL OUTPUT	
WAVELENGTH (nm)	POWER (mW)		
1510	0.4	1510	0.35772
1530	0.4	1530	0.15873
1550	0.42	1550	0.3675
1570	0.38	1570	0.16667
MUX OUTPUT	1.09	MUX OUTPUT	1.0506
EXPERIMENTAL RESULT WITH 85% POWER		MODEL OUTPUT	
1510	0.64	1510	0.57236
1530	0.54	1530	0.21429
1550	0.67	1550	0.58625
1570	0.56	1570	0.24561
MUX OUTPUT	1.6	MUX OUTPUT	1.6185

In the comparison of model and experimental results, it is observed that Equation (31) is comparable to Equation (11) with n' equal to ' l_i ', and ' a_i ' is equal to ' $1/m$ ' for computing wavelength dependent output power of wavelength ' λ_i ' not equal to ' λ_c ', where tolerance limits were taken as 0.5 dBm. For wavelength $\lambda_i = \lambda_c$, ' a_i ' is equal to ' $1.5/m$ '. These power outputs were added together to get the net multiplexer output.

6. CONCLUSION

This paper discusses a mathematical model developed for AWG based multiplexer and demultiplexer based on trigonometric principles. The models are based on the assumption that these devices are linear, and hence the principle of superposition is applied. During the evaluation process of the models, the limitations of the geometrical model have been identified, and an empirical relation obtained from the experimental observations. The empirical relation, which is an approximation to the geometrical model, could compute the AWG power output with a tolerance of 0.5 dBm. Further, these results were validated for various test cases with different input power levels and multiplexer configurations. Since multiplexers play an important role in WDM networks, this proposed model can act as an aid in the construction of optical network model. Thus, it can be used as a basic model for simplifying the analysis of a complex optical WDM network having large number of passive optical components in series.

REFERENCES

1. Van Dam, C., "InP-based polarisation independent wavelength demultiplexers," 1997.
2. Sun, F. G., G. Z. Xiao, Z. Y. Zhang, and Z. G. Lu, "Modeling of arrayed waveguide grating for wavelength interrogation application," *Optics Communications*, Vol. 271, 105–108, 2007.
3. Smit, M. K. and C. Van Dam, "PHASAR-based WDM-devices: Principles, design and applications," *IEEE Journal of Selected Topics in Quantum Electronics*, Vol. 2, No. 2, 236–250, Jun. 1996.
4. Smit, M. K., "New focusing and dispersive planar component based on an optical phased array," *Electronics Letters*, Vol. 24, No. 7, 385–386, 1988.
5. Vellekoop, A. R. and M. K. Smit, "A small-size polarization splitter based on a planar optical phased array," *Journal of Lightwave Technology*, Vol. 8, No. 1, 118–124, 1990.
6. Takahashi, H., S. Suzuki, K. Kato, and I. Nishi, "Arrayed-waveguide grating for wavelength division multi/demultiplexer with nanometre resolution," *Electronics Letters*, Vol. 26, No. 2, 87–88, Jan. 18, 1990, doi: 10.1049/el:19900058.
7. Dragone, C., C. A. Edwards, and R. C. Kistler, "Integrated optics N*N multiplexer on silicon," *IEEE Photonics Technology Letters*, Vol. 3, No. 10, 896–899, Oct. 1991.
8. Zirngibl, M., C. Dragone, and C. H. Joyner, "Demonstration of a 15*15 arrayed waveguide multiplexer on InP," *IEEE Photonics Technology Letters*, Vol. 4, No. 11, 1250–1253, Nov. 1992.
9. Takiguchi, K., K. Okamoto, and A. Sugita, "Arrayed-waveguide grating with uniform loss properties over the entire range of wavelength channels," *Optics Letters*, Vol. 31, No. 4, 459–461, Optical Society of America NTT Photonics Laboratories, 2006.
10. Liu, Z. and J. Li, "Modeling and design of arrayed waveguide gratings," *2nd International Asia Conference on Informatics in Control, Automation and Robotics*, 2010.
11. Roudas, I., N. Antoniadis, T. Otani, and T. E. Stern, "Accurate modeling of optical multiplexer/demultiplexer concatenation in transparent multiwavelength optical networks," *Journal of Lightwave Technology*, Vol. 20, No. 6, 921–936, Jun. 2002.
12. Ab-Rahman, M. S., M. F. Ibrahim, A. A. A. Rahni, S. Shaari, and K. Jumari, "Optical cross add and drop multiplexer: An analytical approach," *The Fourth Advanced International Conference on Telecommunications*, 420–427, 2008, DOI 10.1109/AICT.2008.44.